

TITLE: Anatomical assessment of the eye of the African grasscutter
(*Thryonomys swinderianus*)

SUMMARY

Purpose: To determine the macroscopic and microscopic ocular morphological characteristics of the African grass-cutter

Materials and Methods: Ten male grass-cutters of mean age 4.05 ± 1.44 months and mean weight 1.04 ± 0.56 kg were used for this study. Gross morphologic and light microscopic techniques were employed in the study of the eyes.

Results: Grossly, the eye exhibited typical characteristics of the mammalian eye with a mean eye weight and mean corneal diameter of 0.47 ± 0.14 g and 0.73 ± 0.07 cm, respectively. The horizontal corneal diameter was significantly greater ($p < 0.05$) than the vertical corneal diameter, and the ratio of mean corneal diameter to mean eye diameter (MCD:MED) was 0.80. The sclera and corneal stroma were dense fibrous connective tissues and had thicknesses of $105.3 \pm 25.8 \mu\text{m}$ and $201.4 \pm 91.3 \mu\text{m}$, respectively, while the corneal epithelium was stratified squamous epithelium and measured $50.1 \pm 15.1 \mu\text{m}$. The choroid, ciliary stroma, and iridal stroma were pigmented connective tissues, while the retina was a multi-layered neuro-epithelial tissue with scanty ganglion cells and a retinal pigment epithelium that was pigmented throughout its length.

Conclusion: The high MCD:MED and scanty retinal ganglion cells observed are associated with nocturnal visual capability. However, the complete pigmentation of the retinal pigment epithelium suggest the absence of tapetum lucidum in this species. This could considerably lower its nocturnal visual capability and indicate a low reliance on vision for environmental perception. The biometrical measurements obtained have made data available for use in future ocular studies of the rodent.

32 **Key words:** Ocular morphology, hystricomorpha, rodent,
33 *Thryonomys swinderianus*

34

35 **1. Introduction**

36 The African grasscutter is a nocturnal rodent of the family thryonomidae and
37 suborder hystricomorpha (Igbokwe, 2010). It is usually found in dark
38 environments, such as within lush vegetation and in burrows at daytime. It has
39 gained attention in West Africa as an alternative source of meat and
40 income (Akinola *et al.*, 2015). The increased demand for the meat of this wild
41 rodent aided by its ability to reproduce in captivity have led to the increase in
42 grasscutter farming all over the West African subregion. The sustained growth
43 of this industry may however be impeded by lack of basic knowledge of the
44 biology of the grasscutter. Scientific data on the morphology of the eye of the
45 grasscutter would be useful in its behavioural and medical management,
46 especially in the recognition of ocular pathology.

47 Though numerous studies have been conducted on the grass-cutter (Ajayiet *al.*,
48 2012; Obadiahet *al.*, 2015; Olukole & Obayemi, 2010), studies related to the
49 eye of the rodent are yet very scanty. Therefore, this study sought to describe
50 the ocular characteristics of the African grass-cutter using gross morphologic
51 and light microscopic techniques, and to make available for future reference, its
52 ocular biometric features.

53 **2. Materials and methods**

54 **2.1. Experimental animals**

55 All procedures that involved animals were conducted according to stipulated
56 guidelines for the protection of animal welfare in the University of Nigeria,
57 Nsukka.

58 Ten male African grass-cutters of mean age 4.05 ± 1.44 months and mean
59 weight 1.04 ± 0.56 kg were used for this study. They were obtained from
60 Demacco Farm, Nike, Enugu East Local Government Area, Enugu State,
61 Nigeria, where they were raised in a scarcely illuminated environment.

62 **2.2. Gross anatomy**

63 Following sedation of the rodents using intramuscular injection of xylazine
64 hydrochloride (7 mg/kg), horizontal and vertical corneal diameters were
65 obtained from each eye using Vernier caliper. Euthanasia was subsequently
66 achieved using intramuscular injection of ketamine hydrochloride (120 mg/kg).
67 Eyes were bilaterally enucleated(Hall, 2008) and the eye weight as well as the
68 horizontal, vertical, and axial eye diameters were obtained. The physical
69 appearance and topography of the eyes were studied.

70 **2.3. Light microscopy**

71 Whole eyes were fixed in Davidson's fixative(Agrawal *et al.*, 2007) for 18 hours
72 and subsequently post fixed in 10% neutral buffered formalin. The samples
73 were routinely processed for light microscopy and stained with haematoxylin
74 and eosin (H&E) and Masson's trichrome stains. Photomicrographs were
75 obtained using Moticam Images Plus 2.0 digital camera (Motic China Group
76 Ltd., China) and the **thicknesses of the sclera, cornea and retina were**
77 **measured from one eye of each animal. Due to the varying thicknesses across**
78 **the length of each parameter, five random locations were used for each**
79 **measurement and the means and standard deviations were obtained.**

80 **2.4. Data analysis**

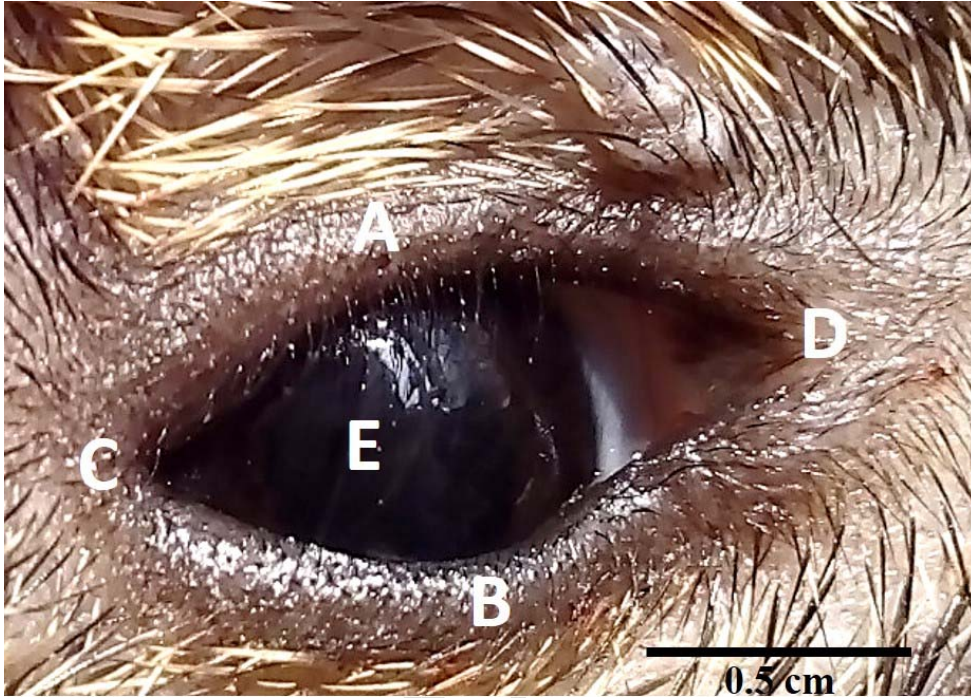
81 Data were analyzed out using SPSS Statistics 17.0 software. Data were
82 presented as mean \pm SD. Mean corneal diameter was calculated as the mean
83 of all horizontal and vertical corneal diameters while mean eye diameter was
84 calculated as the mean of all horizontal and vertical eye diameters. The
85 Wilcoxon signed ranks test was used to determine any significant differences
86 between the vertical and horizontal corneal diameters, vertical and horizontal
87 eye diameters, vertical and axial eye diameters, and axial and horizontal eye
88 diameters. Statistical significance was accepted at $p < 0.05$.

89 **3. Results**

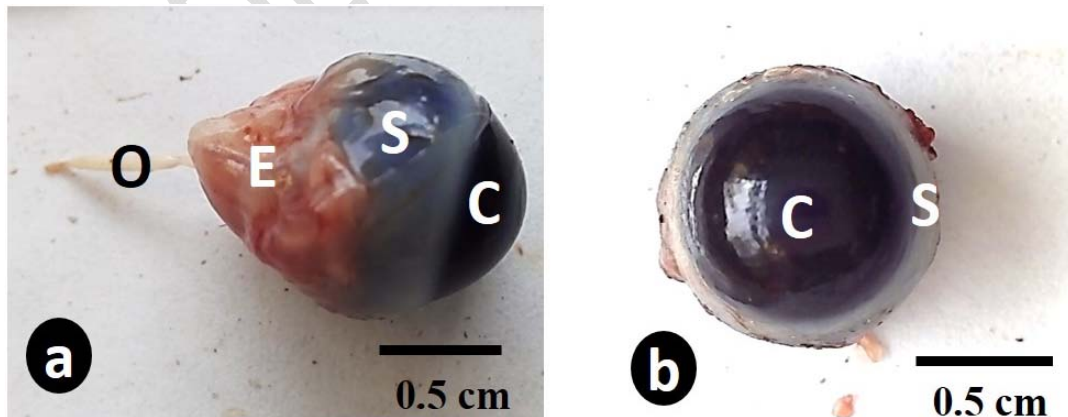
90 **3.1. Gross anatomy**

91 Grossly, the eye exhibited typical characteristics of the mammalian eye (Figure
92 1). Each eye was located laterally in the orbital cavities of the skull with an
93 anterior transparent cornea and a posterior slightly translucent whitish sclera.
94 The sclera was divided into anterior and posterior parts by the whitish

95 translucent conjunctiva, which adhered tightly to the anterior part. Extraocular
96 skeletal muscles were attached to the posterior part. A dark golden-brown iris
97 surrounding a vertically-oriented oval pupil was visible through the cornea. The
98 optic nerve extended from the posterior part of the eye as a white thread-like
99 structure surrounded by extraocular muscles (Figure 2).



100
101 **Figure 1:** Gross photograph of the right eye of *Thryonomyswinderianus*
102 showing typical features of the mammalian eye. Upper eyelid (A), lower eyelid
103 (B), lateral canthus (C), medial canthus (D), eyeball (E).
104



105
106 **Figure 2:** Gross photograph of the enucleated eye of *Thryonomyswinderianus*.
107 Figure 2a shows the equatorial view while figure 2b shows the anterior view.
108 Cornea (C), sclera (S), extraocular muscles (E), optic nerve (O).
109

110 The mean eye weight was 0.47 ± 0.14 g, while the mean corneal diameter was
111 0.73 ± 0.07 cm. The horizontal corneal diameter (0.74 ± 0.08 cm) was
112 significantly greater ($p < 0.05$) than the vertical corneal diameter (0.71 ± 0.05
113 cm). The horizontal eye diameter (0.93 ± 0.07 cm) and axial eye diameter (0.92
114 ± 0.08 cm) were not significantly different ($p > 0.05$) from each other, but were
115 significantly greater ($p < 0.05$) than the vertical eye diameter (0.90 ± 0.09 cm).
116 The ratio of mean corneal diameter to mean eye diameter was 0.80, while the
117 ratio of mean corneal diameter to mean axial eye diameter was 0.79.

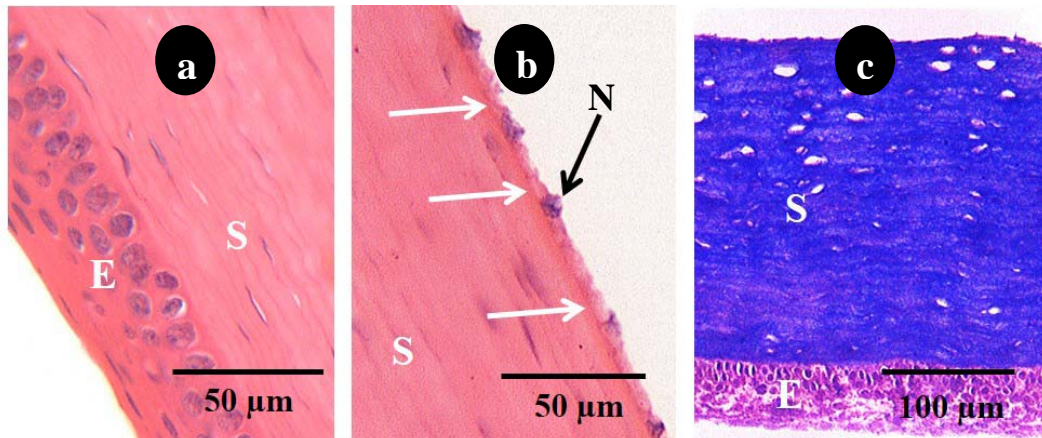
118

119 **3.2. Histology**

120 **3.2.1. Fibrous tunic**

121 The sclera was a dense fibrous connective tissue. It contained numerous
122 fibrocytes and collagen fibers. Pigment cells were scanty and located
123 posteriorly. The cornea appeared as a regular dense fibrous connective tissue
124 (corneal stroma) lined internally by simple cuboidal epithelium (corneal
125 endothelium) and externally by non-keratinized stratified squamous epithelium
126 (corneal epithelium) (Figure 3). The stratified epithelium was 5-12 cell layers
127 thick with round basal cells, oval middle cells and flat apical cells. Unstained
128 perinuclear areas were common among the basal and middle cells. A deeply
129 acidophilic thin area, known as the Descemet's membrane, was observed
130 between the stroma and endothelium (Figure3b). The stroma was filled with
131 closely packed collagen fibers (Figure 3c).The corneal endothelium, stroma,
132 and epithelium made up about 3%, 78%, and 19% respectively of the entire
133 corneal thickness (Table 1).

134



135

136 **Figure 3.** Photomicrograph of the cornea of *Thyronomys swinderianus*. Figures
 137 3a and 3b show the corneal epithelium (E), corneal stroma (S), cells of the
 138 corneal endothelium (N) and the deeply acidophilic, thin Descemet's membrane
 139 (white arrows). Haematoxylin and eosin stain Figure 3c shows the corneal
 140 epithelium (E) and corneal stroma (S) filled with collagen. Masson's trichrome
 141 stain

142

143

144 **Table 1:** Corneal, scleral, and retinal thicknesses of the African grasscutter

	Mean ± SD (µm)	Range (µm)	Percentage
Cornea	257.5 ± 105.9	123.9 - 399.3	-
Corneal endothelium	7.3 ± 1.8	4.9 - 11.2	3%
Corneal stroma	201.4 ± 91.3	86.6 - 329.0	78%
Corneal epithelium	50.1 ± 15.1	25.3 - 74.4	19%
Sclera	105.3 ± 25.8	61.5 - 151.8	-
Retina	140.9 ± 19.4	110.9 - 226.4	-
Retinal piment epithelium	11.1 ± 2.5	7.0 - 16.0	8%
Photoreceptor layer	26.5 ± 7.6	13.3 - 39.7	19%
Outer nuclear layer	31.4 ± 8.0	19.4 - 45.1	22%
Outer plexiform layer	8.1 ± 2.9	4.0 - 12.6	6%
Inner nuclear layer	17.7 ± 3.6	13.0 - 26.7	13%
Inner plexiform layer	24.0 ± 5.2	17.2 - 34.8	17%
Layer of ganglion cells and axons	23.5 ± 3.5	18.1 - 30.1	17%

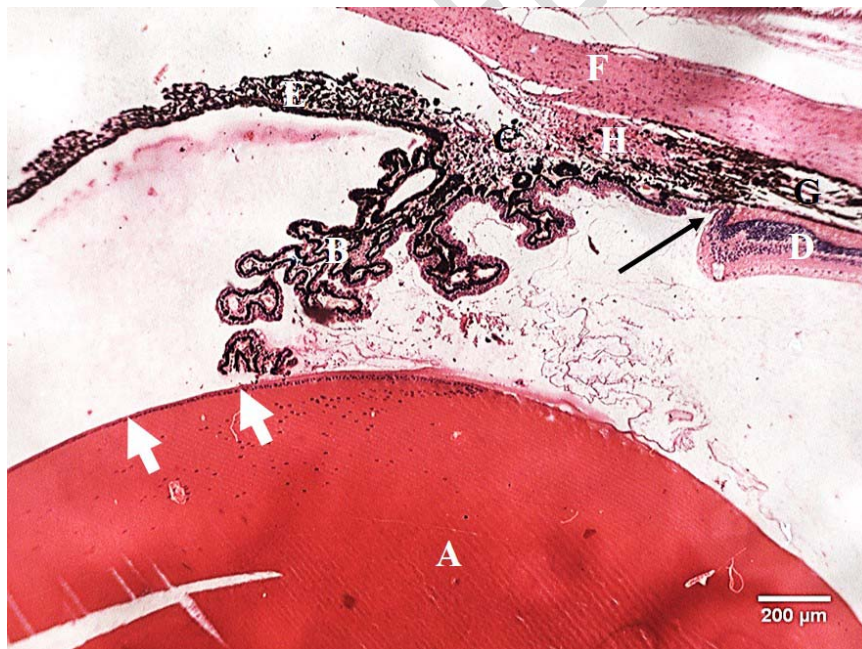
145

146

147

148 **3.2.2. Uvea**

149 The uvea comprised the iris, ciliary body, and choroid. The choroid and ciliary
150 body were separated at the ora serrata (Figure 4). The ciliary body was not well
151 developed. Its stroma, which was continuous with the choroid, was a
152 vascularized pigmented connective tissue layer. Smooth muscle fibers were not
153 observed in the ciliary stroma. The ciliary epithelia consisted of an outer
154 pigmented epithelium and an inner non-pigmented epithelium. The non-
155 pigmented epithelium was simple cuboidal towards the apex of the ciliary
156 processes, but varied from simple columnar to stratified cuboidal towards the
157 base. However, the non-pigmented epithelium gradually accumulated dark
158 brown melanin pigments towards the iris. The connective tissue of the ciliary
159 stroma at the base of the ciliary processes appeared as a meshwork of fibers
160 and cells, the trabecular meshwork (Figure 5). It lacked muscle tissue. Anterior
161 to the ciliary processes was the iris, a long process that extended from the base
162 of the ciliary processes to the space anterior to the lens (Figure 4). It was made
163 up of pigmented connective tissue lined posteriorly by pigmented epithelium
164 that was continuous with the ciliary epithelia.



165

166 **Figure 4.** Photomicrograph of the eye of *Thyronomys swinderianus*. Lens (A),
167 ciliary processes (B), trabecular meshwork (C), retina (D), iris (E), corneoscleral
168 junction (F), choroid (G), ciliary stroma (H), lens epithelium (white arrows), ora
169 serrata (black arrow). Haematoxylin and eosin stain



170

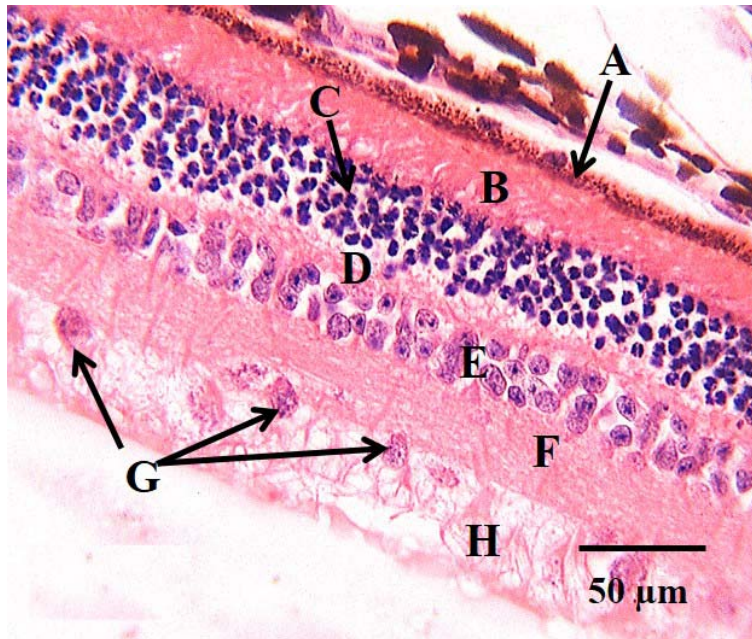
171 **Figure 5.** Photomicrograph of the ciliary body of *Thyronomys swinderianus*.
 172 Corneoscleral junction (J), ciliary processes (P), ciliary stroma filled with
 173 trabecular meshwork (M) and devoid of muscle tissue. Haematoxylin and eosin
 174 stain

175

176 3.2.3. Retina

177 The internal surface of the choroid was lined by multi-layered neuro-epithelial
 178 tissue known as the retina (Figure6). At the base of the retina was a layer of low
 179 simple cuboidal epithelium, the retinal pigment epithelium. The apical three-
 180 quarters of the cytoplasm of the epithelial cells were filled with dark brown
 181 melanin pigments. Beneath this epithelium was an acidophilic layer, the
 182 photoreceptor layer. The outer nuclear layer comprised numerous round
 183 heterochromatic nuclei separated by unstained inter-nuclear spaces (Figure
 184 6). The outer nuclear and photoreceptor layers were the thickest layers of the
 185 retina, occupying about 22% and 19% respectively of the retinal thickness
 186 (Table 1). Two acidophilic layers (outer and inner plexiform layers) were
 187 subjacent to the outer nuclear layer. The outer and inner plexiform layers were
 188 separated by an inner nuclear layer of mostly round euchromatic nuclei and few
 189 elongated euchromatic nuclei. Nuclei of the outer nuclear layer appeared to
 190 make contact with the thin outer plexiform layer through numerous acidophilic
 191 fiber strands. Unstained inter-nuclear spaces were also observed in the inner

192 nuclear layer. The apical layer of the retina contained sparse euchromatic nuclei
193 of ganglion cells dispersed among numerous acidophilic axons. These layers of
194 the retina thinned down abruptly and merged with the ciliary epithelia at the
195 oraserrata.
196



197

198 **Figure 6.** Photomicrograph of the retina of *T. swinderianus*. Retinal pigment
199 epithelium (A), photoreceptor layer (B), outer nuclear layer (C), outer plexiform
200 layer (D), inner nuclear layer (E), inner plexiform layer (F), ganglion cell nuclei
201 (G), axons (H). Haematoxylin and eosin stain
202

203 3.2.4. Lens

204 The lens was a large, deeply acidophilic, circular structure (Figure 4). It was
205 located in the anterior part of the eye between the ciliary processes. A simple
206 cuboidal epithelium, the lens epithelium, lined the anterior surface of the lens
207 while the posterior surface had no epithelial lining. Numerous elongated lens
208 fibers filled the lens.

209

210 4. Discussion

211 Morphology of the cornea of the African grasscutter showed similar features as
212 the cornea of domestic mammals (Hamor & Ehrhart, 2006; Nautscher *et al.*,

213 2016). The closely packed abundant collagen fibers observed in the cornea and
214 sclera of the African grasscutter may serve to provide the tensile strength
215 needed to maintain ocular structural integrity irrespective of fluctuating
216 intraocular pressure. Such amount and arrangement of fibers would prevent
217 rupture of the eyeball in the event of anomalies associated with production and
218 drainage of aqueous humour(Davis *et al.*,2015). The stratified squamous
219 epithelial layer of the corneal epithelium together with the conjunctiva may serve
220 as the anterior protective barrier for the eyeball, since both structures are
221 directly exposed to the external environment. The unstained perinuclear areas
222 observed in the corneal epithelial cells have been demonstrated in the dog, cat,
223 goat, cow, and horse(Hamor & Ehrhart, 2006; Nautscher *et al.*, 2016), but were
224 absent in human cornea(Mescher, 2010; Muller *et al.*, 1995, 1996). These may
225 have been ignored or possibly dismissed as artifacts by previous authors.
226 These unstained areas may not be artifacts, but may require further
227 investigation.

228

229

230

231 The Bowman's membrane of the cornea has been demonstrated in primates
232 and avians(Hamor & Ehrhart, 2006; Mescher, 2010; Muller *et al.*, 1995), but
233 was not observed in the grasscutter. The presence of this membrane in
234 domestic mammals is questionable(Nautscher *et al.*, 2016) and its function is
235 not clearly understood. The ratio of mean corneal diameter to mean eye
236 diameter and that of mean corneal diameter to axial eye diameter were
237 relatively large and comparable to those of nocturnal and cathemeral
238 mammals(Hallet *et al.*, 2012; Kirk, 2004). Such large ratios may increase visual
239 sensitivity(Kirk, 2004) and permit more light rays into the eye at maximum
240 pupillary dilation, unlike in diurnal mammals with smaller ratios(Hall *et al.*,
241 2012). The significantly larger horizontal corneal diameter reported in this study
242 and in most mammals(Augusteyn *et al.*, 2012; Hamor & Ehrhart, 2006; Maggs,
243 2008; Plummer *et al.*, 2003) may be interpreted as an adaptation to minimize
244 energy expended in keeping the eyelids open. We postulate that such an

245 adaptation may allow for entrance of considerable amount of light rays into the
246 eye with minimal exertion of energy by the elevator and depressor muscles of
247 the upper and lower eyelids respectively. The thickness of the corneal
248 epithelium in the grasscutter is small when compared to those of other domestic
249 animals(Nautscher *et al.*, 2016). This may indicate existence of a positive
250 correlation between corneal epithelial thickness and body weight across
251 species.

252 The ciliary body described in this study is similar to that described in rabbits and
253 rodents(Davis, 1929; Woolf, 1956). It was characterized by poorly developed
254 ciliary body and therefore, possible absence of lenticular accommodation.
255 Accommodation nonetheless appears irrelevant to nocturnal animals in which
256 visual sensitivity takes pre-eminence over visual acuity. Ciliary muscle fibers
257 have however been reported in the mouse(Treuting *et al.*, 2012). The presence
258 of melanin pigments in the non-pigmented epithelium of the ciliary body at the
259 para-iridal area suggests that this area may be a transition zone between the
260 ciliary body and the iris. Thus, the term, 'non-pigmented epithelium' appears
261 unsuitable for this area.

262 The sum of the percentages of the various retinal components was about 102%
263 instead of 100% due to errors in the subjective determination of the
264 measurements. This was because the entire retinal thickness stated was not a
265 direct numerical computation of the thicknesses of its components but was
266 rather measured alongside its components. The retinal pigment epithelium in the
267 grasscutter exhibited melanin pigments throughout its length. In mammals with
268 tapetumlucidum, the retinal pigment epithelium usually lacks melanin pigments
269 over the central area of the tapetum(Ollivier *et al.*, 2004). The presence of
270 pigments throughout the tapetum therefore suggests the absence of tapetum
271 lucidum in the grasscutter. Tapetumlucidum has been reported to be absent in
272 most rodents except the spotted cavy (*Cuniculus paca*) and the springhaas
273 (*Pedetes capensis*)(Fernandez & Dubielzig, 2013).It is a reflective structure of
274 the eye that improves night vision in nocturnal, cathemeral and crepuscular
275 animals.

276

277

278

279 The sparse ganglion cells in the retina of the grasscutter indicate poor visual
280 acuity in this species. This feature, known as retinal pooling(Hall, 2008), has
281 been associated with nocturnal animals.

282 In photopic animals such as humans, there is a higher density of ganglion cells,
283 and consequently, high visual acuity(Vajzovic *et al.*, 2012).

284 **5. Conclusion**

285 In conclusion, the visual system of the African grasscutter is adapted for
286 nocturnal vision as suggested by the high ratio of mean corneal diameter to
287 mean eye diameter and scanty retinal ganglion cells. This nocturnal visual
288 capability may however be considerably lowered by the absence of
289 tapetumlucidum as suggested in this species.**The biometrical measurements**
290 **obtained has made data available for use in future ocular studies of the rodent.**

291

292 **Disclaimer regarding Consent and Ethical Approval:**

293 As per university standard guideline, participant consent and ethical approval
294 have been collected and preserved by the authors.

295 **References**

296 Agrawal, R. N.; He, S.; Spee, C.; Cui, J. Z.; Ryan, S. J. & Hinton, D. R. In vivo
297 models of proliferative vitreoretinopathy. *Nat. Protoc.*, 2(1):67–77, 2017

298 Ajayi, I. E.;Shawulu, J. C. &Nafarnda, W. D. Organ Body Weight Relationship of
299 Some Organs in the Male African Grasscutter (*Thryonomyswinderianus*).
300 *J. Adv. Vet. Res.*, 2:86–90, 2012.

301 Akinola, L. A. F.;Etela, I. &Emiero, S. R. Grasscutter (*Thryonomyswinderianus*)
302 production in West Africa: Prospects, Challenges and Role in Disease
303 Transmission. *Am. J. Exp. Agric.*, 6(4):196–207, 2015.

304 Augusteyn, R. C.; Nankivil, D.; Mohamed, A.;Maceo, B.; Pierre, F. &Parel, J.
305 Human ocular biometry. *Exp. Eye Res.*, 102:70–75, 2012.

306 Davis, F. A. The anatomy and histology of the eye and orbit of the rabbit. *Trans.*
307 *Am. Ophthalmol. Soc.*, 27:400–441, 1929.

308 Davis, K.; Carter, R.; Tully, T.;Negulescu, I.& Storey, E. Comparative evaluation
309 of aqueous humor viscosity. *Vet. Ophthalmol.*, 18(1):50–58, 2015.

310 Fernandez, J. R. &Dubielzig, R. R. Ocular comparative anatomy of the family
311 Rodentia. *Vet. Ophthalmol.*, 16:94–99, 2013.

312 Hall, M. I. Comparative analysis of the size and shape of the lizard eye.
313 *Zoology*, 111:62–75, 2008.

314 Hall, M. I.; Kamlar, J. M.& Kirk, E. C. Eye shape and the nocturnal bottleneck of
315 mammals. *Proc. R. Soc. B*, 279:4962–4968, 2012.

316 Hamor, R. E.&Ehrhart, E. J. Eye. In Eurell, J. A &Frappier, B. L (Eds.),
317 Dellmann's Textbook of Veterinary Histology (6th ed., pp. 350–363).
318 Blackwell Publishing Ltd., 2006.

319 Igbokwe, C. O. Gross and microscopic anatomy of thyroid gland of the wild
320 African grasscutter (Thryonomyswinderianus, Temminck) in Southeast
321 Nigeria. *Eur. J. Anat.*, 14(1):5–10, 2010.

322 Kirk, E. C. Comparative Morphology of the Eye in Primates. *Anat. Rec.*,
323 281A:1095–1103. 2004.

324 Maggs, D. J. *Cornea and Sclera*. In Maggs, D. J.; Miller, P. E. &OfriR. (Eds.),
325 Slatter's Fundamentals of Veterinary Ophthalmology (4th ed., pp. 175–
326 202). Saunders Elsevier, 2008.

327 Mescher, A. L. *Junqueira's Basic Histology* (12th ed.). McGraw-Hill, 2010.

328 Muller, L. J.;Pels, L. &Vrensen, G. F. J. M. Novel Aspects of the Ultrastructural
329 Organization of Human Corneal Keratocytes. *Invest. Ophthalmol. Vis. Sci.*,
330 36(13):2557–2567, 1995.

331 Muller, L. J.;Pels, L.&Vrensen, G. J. M. Ultrastructural Organization of Human
332 Corneal Nerves. *Invest. Ophthalmol. Vis. Sci.*, 37(4):476–488, 1996.

333 Nautscher, N.; Bauer, A.;Steffl, M.&Amselgruber, W. M. Comparative
334 morphological evaluation of domestic animal cornea. *Vet.Ophthalmol.*,
335 19:297–304, 2016.

336 Obadiah, B.; Dzenda, T. & Happiness, O. I. Tail Allometry of the Grasscutter
337 (Thryonomyswinderianus) and African Giant Pouched Rat
338 (Cricetomysgambianus): It's Functional Relevance. *World J. Zool*,
339 10(2):112–117, 2015.

340 Ollivier, F. J.; Samuelson, D. A.; Brooks, D. E.; Lewis, P. A.; Kallberg, M. E.
341 &Komáromy, A. M. Comparative morphology of the tapetumlucidum
342 (among selected species). *Vet. Ophthalmol.*, 7(1):11–22, 2004.

343 Olukole, S. G. &Obayemi, T. E. Histomorphometry of the Testes and Epididymis
344 in the Domesticated Adult African Great Cane Rat
345 (*Thryonomys swinderianus*). *Int. J. Morphol.*, 28(4), 1251–1254, 2010.

346 Plummer, C. E.; Ramsey, D. T. & Hauptman, J. G. Assessment of corneal
347 thickness, intraocular pressure, optical corneal diameter, and axial globe
348 dimensions in Miniature Horses. *Am. J. Vet. Res.*, 64(6):661–665, 2003.

349 Treuting, P. M.; Wong, R.; Tu, D. C. & Phan, I. *Special Senses: Eye*. In
350 Treuting P. M. & Dintzis S. M. (Eds.), *Comparative Anatomy and Histology*
351 (pp. 395–418). Elsevier Inc., 2012.

352 Vajzovic, L.; Hendrickson, A. E.; O'Connell, R. V.; Clark, L. A.; Tran-Viet,
353 D.; Possin, D.; Chiu, S. J.; Farsiu, S. & Toth, C. A. Maturation of the Human
354 Fovea: Correlation of Spectral-Domain Optical Coherence Tomography
355 Findings With Histology. *Am. J. Ophthalmol.*, 154(5):779–789, 2012.

356 Woolf, D. A comparative cytological study of the ciliary muscle. *Anat. Rec.*,
357 124(2), 145–163, 1956.

358

359